Ocean Engineering 142 (2017) 532–540

Contents lists available at ScienceDirect

Ocean Engineering

journal homepage: www.elsevier.com/locate/oceaneng

Numerical simulation of ultra-high speed supercavitating flows considering the effects of the water compressibility

Changchang Wang, Guoyu Wang*, Mindi Zhang*, Biao Huang, Deming Gao

School of Mechanical and Vechicular Engineering, Beijing Institute of Technology, 5 South Zhongguancun Street, Beijing 100081, China

ARTICLE INFO

Keywords:
Water compressibility effects
Subsonic
Transonic
Supersonic
Supercavity shape

ABSTRACT

The objective of this paper is to address the simulation of supercavitating flows around a slender body projectile at the sub-, trans- and supersonic speeds with the water compressibility effects considered. Based on the slender body theory (SBT) and the matched asymptotic expansion method (MAEM), the integro-differential equations for the cases of $M_a < 1$ and $M_a > 1$ are derived and solved. The results show that there is a good agreement of the supercavity shape for both the cases of $M_a < 1$ and $M_a > 1$ between the numerical simulation and the experimental results. The influence of Mach number on the supercavity length L, maximum radius R, slenderness λ, the corresponding growth rate of the supercavity length $\tilde{L}$, the growth rate of the maximum supercavity radius $\tilde{R}$, and the position of the supercavity maximum section (PSMS) are discussed. It can be found that $\tilde{L}$ is much bigger than $\tilde{R}$, due to the large λ. It also concludes that the front part of the supercavity is thicker than the rear part, and the PSMS moves forward further at supersonic speed. Finally, the reason for the supercavity shape transition around $M_a = 1$ is illustrated and it may be the c$_a$use of the extension of perturbation zones at transonic speed.

1. Introduction

Low-subsonic to supersonic ultra-high speed supercavitating underwater projectiles can be used for underwater mine neutralization, surf zone mine clearance and other defensive warfare application. For such ultra-high speeds, the water compressibility effects cannot be ignored. Numerous researches (Chen et al., 1985; Owis and Nayfeh, 2003; Gu et al., 2005; Ohtani et al., 2006; Passandiedeh-Fard and Roohi E, 2008) have been conducted on the supercavitating underwater projectile below the speed of 100 m/s. However, the researches on ultra-high speed supercavitating flows around a slender body from low-subsonic to supersonic speed is not enough. Thus, it is necessary to investigate the ultra-high speed supercavitating underwater projectile considering the water compressibility effects.

Due to the complexity, the high cost and the military reasons of experimental researches at high speeds, only few of experiments have been published on high speed supercavitating projectiles. Vlasenko (2003) conducted experimental investigations of hydrodynamics of supercavitating projectiles moving in water at velocities from low subsonic speed to sonic speed. He described the qualitative features of the ultra-high speed supercavities and the water compressibility effects in the zone in front of the cavitator at motion regimes with Mach numbers in the range of $M_a = 0.54–0.77$. Furthermore, an empirical formula validated in the velocity rage $v = 40–1300$ m/s was obtained to calculate the shape and dimensions of the axisymmetric supercavities, and it was found that the experimental data was in good agreement with the empirical formula. Hrubes (2000) applied high-speed imaging techniques in an underwater environment to provide images essential to the understanding of the launch and flight of underwater supercavitating projectiles. The images revealed information on projectile flight behavior, stability mechanisms, cavity shape, and in-barrel launch characteristics. In the supersonic tests, projectile shock waves were revealed. In order to better understand the high speed supercavitating projectile flight and stability in flows over a range of cavitation numbers and underwater Mach numbers from zero through and exceeding unity, Kirschner (2001) made quantitative measurements to determine the projectile velocity time history, projectile drag, projectile trajectory, and spatial and temporal characteristics of the cavity. Yamashita et al. (2004) conducted experiments to visualize and analyze the motion of the spherical shaped projectile and slender shaped projectile to investigate the ultra-high speed supercavitating phenomenon, which are launched into the water under the supersonic condition at velocity ranging from 1500 m/s to 2000 m/s. By analyzing the sequential images, they found that, the initial shock wave generated by the projectile impact propagates approximately at the speed of sound and also confirmed the effect of the supercavitation on drag

* Corresponding authors.
E-mail addresses: wangguoyu@bit.edu.cn (G. Wang), zmd1971@bit.edu.cn (M. Zhang).

http://dx.doi.org/10.1016/j.oceaneng.2017.07.041
Received 22 July 2016; Received in revised form 13 March 2017; Accepted 11 July 2017

reduction compared to the single phase flow successfully.

There are three ways to numerically simulate the high-speed supercavitating flow, namely viscous flow theory, empirical method and potential flow theory.

Kunz et al. (2001), and Lindau et al. (2003a, 2003b) developed the multiphase computational fluid dynamics (CFD) methods to simulate the viscous, rotational two-phase supercavitating flows. However, due to a range of complex physical phenomena, including viscous effects, unsteadiness, mass transfer, three-dimensionality and especially the compressibility effects, the CFD method demands rigorous computational conditions. Recently, based on the mixture model and user defined function in CFD code Fluent 6.3, Zhang and Fu (2009) simulated numerically both of the incompressible and compressible flow field of supercavitating flows from subsonic to supersonic underwater. The results showed the temperature distribution around the projectile. They also found that the compressibility effects of water can increase drag of projectile and generate lots of heat. Yi et al. (2008), using the Fluent software, calculated the supercavity shapes behind the disk and coniform cavitators and analyzed the influences of cavitation number, headforms, half cone angle and cavitator diameters on supercavity shape. The results showed that the ratio of length to diameter of supercavity behind the underwater projectile is very large and reduces rapidly with the increase of cavitation number. Saranjam (2013) used unsteady Reynolds averaged Navier-Stokes equations coupled with a six-degree-of-freedom to simulate and predict unsteady cavitation shape, dynamics behavior and trajectory of the moving object and acted forces on the body. The results illustrated that the numerical algorithm can be used for the supercavitating underwater vehicles optimization and performance analysis. Roohi et al. (2015) (Pendar and Roohi, 2016) compared different turbulence and mass transfer models over a broad range of cavitation number especially in small cavitation numbers under the framework of the OpenFOAM package and presented a correlation between the cavity length and diameter for hemispherical head-form bodies. The empirical method is comparatively simple and has been used widely and successfully to model developed cavitation. Based on the principle of independence of the cavity sections expansion and experimental data under low speed, some researchers (Garabedian, 1956; Logvinovich, 1973; Savcheko, 1998) concluded a few popular empirical formulas. These formulas are convenient for the low speed, however, when the projectile speed reaches the speed of sound, more complex phenomena requires new method. Adapting the potential theory, Nouri and Eslamdoost (2009) developed an iterative scheme using the boundary element method (BEM) to simulate the supercavitating potential flows. Results showed that the scheme was reliable and could be applied to predict the characteristics of a supercavitating flow and also had the ability to capture the cavity in a flow field with low cavitation number. Based on the slender body theory (SBT) and matched asymptotic expansion method (MAEM), Vasin (1998, 2001a, 2001b) and Zhang et al. (2015) solved subsonic and supersonic flows using finite difference method (FDM) according to the Laplace equation. However, the practicability of FDM is limited especially for complex boundary conditions, and its conservation should be improved. Semenenko (1997, 2001a, 2001b) and Pellone et al. (2004) developed a self-program to simulate the unsteady supercavitating flow based on the principle of independence of the cavity sections expansions. Vladimir et al. (2003), Serebryakov (2006) and Serebryakov et al. (2009) established several models for the prediction of supercavity shape for both of incompressible and compressible water adopting the parameter k and μ for sub-, trans- and supersonic flow. They demonstrated that in the transonic case (0.7 $< M_\infty <$ 1.5), the phenomenon that cavity length and radius increase sharply and then decrease sharply is the result of the significant increase of the extension of the perturbation zone. Zhang et al., (2010, 2011) improved the accuracy of supercavity shape, and analyzed the effects of water compressibility on the high-speed supercavity shape.

Although many important advances have been made in the numerical simulation of ultra-high speed supercavitating flows in above works, some issues about the supercavity shape in ultra-high sonic speed considering water compressibility have not been resolved yet. In the present study, an analytical asymptotic method based on the slender body theory (SBT) and matched asymptotic expansion method (MAEM), with the water compressibility effects considered, is applied for the simulation of the supercavitating flows around a slender body at the sub-, trans-and supersonic speed cases under small cavitation number ranging from 10^{-3} to 10^{-5}. According to the simulation results, the influence of velocity on the predicted supercavity length L, maximum supercavity radius R, slenderness λ, the corresponding growth rate of the supercavity length $\widetilde{L}$, the growth rate of supercavity maximum supercavity radius $\widetilde{R}$ and the position of the supercavity maximum section (PSMS) are discussed.

2. Numerical model

2.1. Governing equations based on slender body theory (SBT)

Considering a steady flow around a fixed slender body in an unbounded, ideal compressible fluid, the cylindrical coordinate system (r, x) is chosen, as shown in Fig. 1. It is assumed that the fluid is inviscid and that the flow is irrotational. Then, the steady irrotational compressible potential flow equation for a Newtonian fluid, linearized based on the small disturbance theory, is presented below (Vladimir et al., 2003).

$$\frac{\partial^2\varphi}{\partial r^2} + (1 - M_a^2)\frac{\partial^2\varphi}{\partial x^2} + \frac{\partial\varphi}{r\partial r} = 0 \tag{1}$$

The Tait state equation (Cole, 1948) is applied to describe the state of the water as follows:

$$\frac{p + B}{\rho^n} = \frac{p_\infty + B}{\rho_\infty^n} \tag{2}$$

Where φ is the flow potential of perturbations, $M_a = u_\infty/c_\infty$, u_∞ is the free stream velocity, c_∞ is the speed of sound in the undisturbed flow, B = 2985 bar, n = 7.15, $p \leq$ 3 GPa (Zamyshlyaev and Yakovlev, 1973), and the subscript represents the infinite parameter. Eq. (2) is valid under the condition of $M_a <$ 2.2 and the flow is assumed isentropic and potential. It gives the possibility to derive a compressible Bernoulli equation and the sonic speed of water (Cole, 1948).

$$\frac{n}{n-1}\frac{p + B}{\rho} + \frac{(U_\infty + u)^2 + v^2}{2} = \frac{n}{n-1}\frac{p_\infty + B}{\rho_\infty} + \frac{U_\infty^2}{2} \tag{3}$$

$$a^2 = \frac{dp}{d\rho} = \frac{n(p + B)}{\rho} \tag{4}$$

Here, u and v are the axial and radial perturbation velocities along streamlines, respectively.

In the present method, the Riabushinsky closure scheme for the back of the cavity is used. For a given cavitator shape, $r = r(x)$, the impenetrability condition is described as follows:

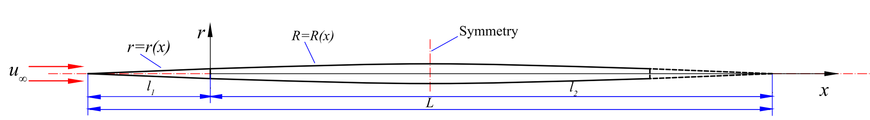

Fig. 1. Schematic of supercavitating flows around a slender body.